Thin-Walled Structures 75 (2014) 30–42

Contents lists available at ScienceDirect

Thin-Walled Structures

journal homepage: www.elsevier.com/locate/tws

# Seismic behavior of steel plate shear walls with centrally placed circular perforations

Anjan K. Bhowmick*

*Department of Building, Civil and Environmental Engineering, Concordia University, Montreal, Quebec, Canada*

ARTICLE INFO

*Article history:*
Received 14 December 2012
Received in revised form
24 June 2013
Accepted 10 September 2013

*Keywords:*
Steel plate shear wall
Seismic analysis
Circular perforations
Unstiffened thin plate

ABSTRACT

The behavior of unstiffened thin steel plate shear walls with circular perforations placed at the center of the infill plates is examined. A shear strength equation is developed for perforated steel plate shear wall with circular perforation at the center. A series of single storey perforated steel plate shear walls with different aspect ratios and different perforation diameters were analyzed to assess the proposed shear strength equation. A comparison between the nonlinear pushover analysis and the proposed equation shows excellent agreement. The proposed shear strength equation is applied for design of boundary columns of one 4-storey and one 6-storey perforated steel plate shear walls. The predicted design forces in the boundary columns for the selected perforated shear walls are compared to the forces obtained from nonlinear seismic analysis. The proposed equation gives very good predictions for the design forces in the boundary columns.



## 1. Introduction

Steel plate shear walls (SPSWs) are a very effective system for resisting lateral loads due to wind and earthquakes. A properly designed SPSW has high ductility, high initial stiffness, high redundancy, and excellent energy absorption capacity in comparison to many conventional lateral load resisting systems. Steel plate shear walls are also lighter and more ductile than reinforced concrete shear walls and they are relatively easy to install. In North America, the current practice is to use thin unstiffened steel plates for the infill plates, relying on post-buckling strength of the infill plates to calculate the capacity of SPSWs. The surrounding framing members are generally "capacity designed", i.e., designed to develop the infill plate tension field capacity, while themselves remaining essentially elastic.

Because of the efficiency of the infill plate in carrying storey shears, it has been observed [1] that plate thickness requirements in SPSWs are generally very low, especially for mid to low-rise buildings, even under relatively severe seismic loading. Very often, in some SPSW applications, the minimum panel thicknesses available from steel producers are much thicker than that required by the design. Use of larger than required infill plate thickness introduces a problem in capacity design, as this will introduce excessive forces to the surrounding frame members, thus increasing their required size as per capacity design. Recently, attempts have been made to address this problem by (a) using light-gauge cold-formed steel infill plates instead of regular hot-rolled infill plates [2,3], (b) using low yield strength (LYS) steel for infill plates [3], (c) introducing vertical slits in the infill plate [4,5], (d) connecting the infill plate only with the beams in a moment frame of SPSW system [6], or (e) introducing a regular pattern of circular perforations in the infill plate [3]. Among all the proposed options, the perforated SPSW recommended by Vian [3], shown in Fig. 1, represents an attractive system since it can also accommodate the need of utility systems to pass through the infill plates.

Research on circular perforations in shear panels similar to SPSWs started with Roberts and Sabouri-Ghomi [7]. They conducted a series of quasi-static tests under cyclic diagonal loading on unstiffened steel plate shear panels with centrally-placed circular perforations. Based on the results, the researchers proposed the following approximate equation for strength of an unstiffened infill panel with a central circular opening

$$V_{op} = V_p\left(1-\frac{D}{d_p}\right) \tag{1}$$

where $V_{op}$ and $V_p$ are the strength of a perforated and a solid shear panel, respectively, $D$ is the perforation diameter, and $d_p$ is the panel height. The equation proposed by Roberts and Sabouri-Ghomi [7] was only tested for relatively small rectangular and square shear panel specimens (maximum size: 450 mm × 300 mm) loaded in shear.

Purba [8] analyzed a 4000 mm by 2000 mm single storey SPSW with multiple regularly-spaced circular perforations of equal diameter. It was observed that for multiple regularly-spaced perforations, Eq. (1)

* Tel.: +1 514 848 2424; fax: +1 514 848 7965.
*E-mail address:* anjan.bhowmick@concordia.ca

0263-8231/$ - see front matter © 2013 Elsevier Ltd. All rights reserved.
http://dx.doi.org/10.1016/j.tws.2013.09.027

**Nomenclature**

| | |
|---|---|
| $A_{bi}$ | $i$thbeam cross-sectional area. |
| $D$ | Perforation diameter. |
| $d_p$ | Panel height. |
| $F_y$ | Yield strength. |
| $F_{yb}$ | $i$thbeam yield strength. |
| $I_c$ | Moment of inertia of each column. |
| $P_b$ | Axial forces in beams. |
| $R_y$ | Ratio of the expected steel yield stress to the nominal yield stress. |
| $S_{diag}$ | Diagonal distance between each perforation line. |
| $V_{op}$ | Shear strength of perforated plate. |
| $V_p$ | Shear strength of solid plate. |
| $w$ | Infill plate thickness. |
| α | Angle of tension field. |
| $\omega_h$ | Column flexibility parameter. |
| $\omega_{xci}$ | Distributed loads ($x$-component) from plate yielding applied to the $i$thcolumn |
| $\omega_{yci}$ | Distributed loads ($y$-component) from plate yielding applied to the $i$thcolumn. |
| $\omega_{bi}$ | Distributed loads from plate yielding applied to the $i$thbeam. |
| $\omega_{xbi}$ | Distributed loads ($x$-component) from plate yielding applied to the $i$thbeam. |
| $\omega_{xbi+1}$ | Distributed loads ($x$-component) from $(i+1)$thplate yielding applied to the $i$thbeam. |
| $\omega_{xbi-1}$ | Distributed loads ($x$-component) from $(i-1)$thplate yielding applied to the $i$thbeam. |
| $\omega_{ybi}$ | Distributed loads ($y$-component) from plate yielding applied to the $i$thbeam. |
| $\omega_{ybi-1}$ | Distributed loads ($y$-component) from $(i-1)$thplate yielding applied to the $i$thbeam. |
| $\omega_{ybi+1}$ | Distributed loads ($y$-component) from $(i+1)$thplate yielding applied to the $i$thbeam. |
| $L_{p,eff}$ | Effective width of the perforated infill plate. |
| $L_p$ | Width of perforated infill plate. |
| $M_{col,i}$ | Moment at $i$thcolumn. |
| $M_{pri}$ | Reduced plastic moment capacity at the ends of beam $i$. |
| $P_{b(col)}$ | Beam axial force, contribution from column with inward infill plate forces applied to it. |
| $P_{b(plate)}$ | Beam axial force, contribution from difference in infill plate's forces above and below the beam. |
| $V_{bi}$ | Shear forces at the ends of beam $i$. |
| $Z_{xi}$ | Beam plastic section modulus. |

provides a conservative estimate of the strength of the perforated infill plate when $d_p$ in Eq. (1) is replaced by $S_{diag}$, the diagonal distance between each perforation line (see Fig. 1). Through a calibration study, the following modified equation was proposed to calculate the shear strength of perforated SPSWs with the regular perforation pattern used by Vian [3]:

$$V_{op} = V_p\left(1 - 0.7\frac{D}{S_{diag}}\right) \tag{2}$$

Although Eq. (2) was found to provide good strength predictions of SPSWs for the regular perforation pattern proposed by Vian [3], very often engineers want to place only a single larger opening at the center of the infill plate. This is mainly for ease of fabrication. A single perforation at the center of the infill plate would significantly reduce the cost of fabrication in compare to the existing regularly spaced perforation layout. Currently there are no guidelines available to design SPSWs with a single circular opening at the center of the shear walls.

This paper presents a simple equation for determining the strength of perforated SPSWs with centrally located circular perforations. The proposed equation is based on a strip model concept, and is derived by discounting the strip that is intercepted by the perforation. Finite element models of three single storey SPSWs (with aspect ratios of 2.0, 1.5, and 1.0) with nine different types of perforation diameters are analyzed to investigate the effectiveness of the proposed equation.

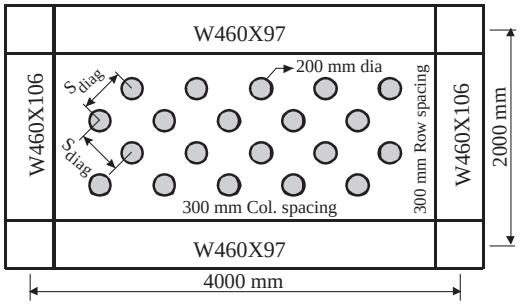


**Fig. 1.** Perforation layout of test specimen from Vian [3].

AISC Steel Design Guide 20 [9] presents a capacity design method for the design of SPSW columns with solid infill plates. The method in AISC Steel Design Guide 20 [9] assumes that all the infill plates over the building height reach their full yield capacity, and plastic hinges are assumed at the ends of all the horizontal members of the frame. Forces from the infill plate tension fields and the force effects from the beams are then applied to free body diagrams of the boundary columns to determine their design axial forces and moments. The presence of perforations in the infill plates affects the axial forces and moments in the boundary columns, thus requiring modifications to the current design method. This paper presents modifications to the capacity design method of AISC Steel Design Guide 20 [9] to accommodate SPSWs with centrally located circular perforations. With the modifications in the current capacity design method, columns of one 4-storey and one 6-storey perforated SPSWs with centrally placed circular perforations are designed. The resulting design forces for the boundary columns are compared with the design forces obtained from seismic analysis of the selected SPSWs under site specific earthquake ground motions for Vancouver, Canada.

## 2. Strength equation for infill plate with centrally located perforation

To develop a general strength model, it is assumed that the shear strength of the SPSW is provided strictly by tension field action in the infill plate. The angle of the tension field, $\alpha$, is obtained from the equation specified both in Canadian standard, CAN/CSA-S16-09 [10] and AISC seismic Specification [11]. It is assumed that in the presence of a circular hole of diameter $D$, as shown in Fig. 2, one can discount the steel within a diagonal strip of width $D$. This assumption will be investigated by conducting series of finite element analysis. If the diagonal strip containing the circular hole is at an angle $\alpha$, angle of tension field, the horizontal projection of the portion of the strip to be discounted is $D/\cos\alpha$. After discounting the strip with the circular perforation, the effective width of the perforated infill plate,

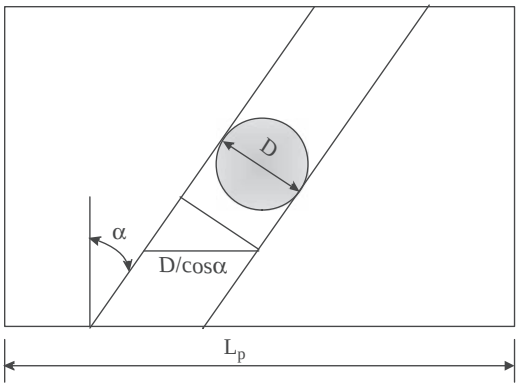


**Fig. 2.** Strip model representation for centrally perforated infill plate.

$L_{p,eff}$, becomes

$$L_{p,eff} = L_p - \frac{D}{\cos\ \alpha} \tag{3}$$

where $L_p$is the width of perforated infill plate.

The shear strength of a solid infill plate, $V_p$, is given by [12]

$$V_p = 0.5\sigma\ wL_p\ \sin\ 2\alpha \tag{4}$$

where $w$ is the infill plate thickness and $\sigma$ is the stress in the infill plate (remaining solid) tension strips, taken as the yield stress for design.

Thus, the shear strength of a perforated infill plate, $V_{op}$ is

$$V_{op} = 0.5\sigma\ w\left(L_p - \frac{D}{\cos\ \alpha}\right)\ \sin\ 2\alpha \tag{5}$$

From Eqs. (4) and (5)

$$\frac{V_{op}}{V_p} = \left(1 - \frac{D}{L_p\ \cos\ \alpha}\right) \tag{6}$$

In the next section, a series of single-storey SPSWs with different aspect ratios and different perforation diameters are analyzed to investigate the applicability of the proposed equation.

## 3. Analysis of perforated steel plate shear walls

Nonlinear finite element analyses of a series of single-storey SPSWs with centrally located circular perforations were carried out using ABAQUS [13]. Both material and geometric nonlinearities were considered. In total, nine different types of perforation diameters were considered in this study.

### 3.1. Selection of the shear wall system

The single-storey perforated steel plate shear walls considered in this study are part of a hypothetical symmetrical office building located in Vancouver, Canada. The building has a total area of 2014 $m^2$ and has height of 3.8 m. As shown in Fig. 3, the building has two identical SPSWs to resist lateral loads in each direction. For simplicity, each shear wall was assumed to resist one half of the design seismic loads. Three different aspect ratios of 1.0, 1.5 and 2.0 are considered for this study. Thus the shear walls have width of 3.8 m, 5.7 m and 7.6 m, measured from center to center of columns. The building was assumed to be located on dense soil or soft rock (site class C according to National Building Code of Canada, NBC 2010). A dead load of 1.12 kPa was used for the roof. The snow load at the roof was taken as 1.48 kPa. NBC 2010 [14] load combination $D+0.5L+E$ (where $D$=dead loads, $L$=live loads and $E$=earthquake loads) was considered for

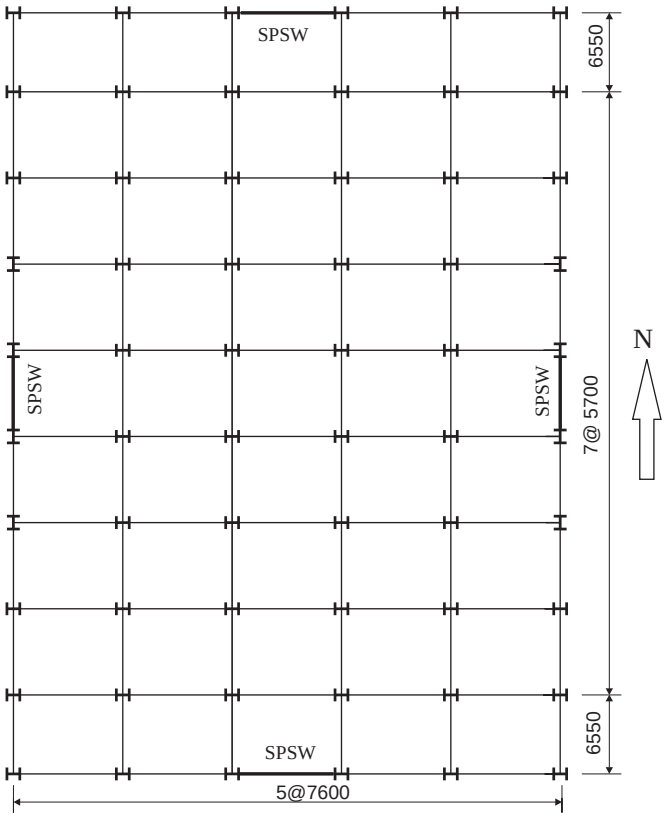


**Fig. 3.** Plan view of sample building.

intermediate floors and for the roof, the load combination $D+0.25S+E$ (where $S$=snow loads) was considered. Design seismic load was calculated using the equivalent static force procedure of the NBC 2010. An importance factor, $I$, of 1.0 was selected for the design. As prescribed by NBC 2010, a ductility-related force modification factor,$R_d$, of 5.0 and an overstrength force modification factor, $R_o$, of 1.6 were used in the design.

An infill plate thickness of 3.0 mm was used, as this is considered the minimum practical thickness using conventional welding practice and for handling considerations. Shishkin et al. [15] observed that the ultimate base shears of SPSWs varied little when the angle of inclination of the tension field, $\alpha$, was changed from 38° to 50°. Also, at the beginning of design of any SPSW, the column sections are unknown to determine the angle of tension field. Thus, the value of the angle of the diagonal tension field was assumed as 45° in this paper. With the angle of the tension field known, boundary beams and columns were selected. The top and bottom beams were selected to anchor the tension forces from the yielded infill plate. Also the column sections were selected to carry the forces developed in the yielded infill plate and the plastic hinges at the ends of the top beams. CAN/CSA-S16-09 also has provisions for the stiffness of the columns to ensure the development of an essentially uniform tension field in the infill plate. The required limit on the flexibility parameter, $\omega_h$, is given as

$$\omega_h = 0.7h\sqrt[4]{\frac{w}{2LI_c}} \le 2.5 \tag{7}$$

where $w$ is the infill plate thickness; $L$ is the bay width; $h$ is the storey height; and $I_c$is the moment of inertia of each column.

Table 1 presents the selected beams and columns sections for the three selected shear walls. Nine different perforation diameters were considered for each selected shear wall.

**Table 1**
Summary of 1-storey perforated SPSWs properties.

| Aspect ratio | Plate thickness (mm) | Column section | Top/bottom beam section |
|---|---|---|---|
| 1.0 | 3 | W360 × 382 | W530 × 150 |
| 1.0 | 1 | W310 × 143 | W410 × 74 |
| 1.5 | 3 | W360 × 509 | W530 × 272 |
| 2.0 | 3 | W360 × 900 | W610 × 498 |

### 3.2. Characteristics of the finite element model

The infill plate and boundary members (beams and columns) were modeled using a general purpose four-node, doubly-curved, shell element with reduced integration (ABAQUS element S4R). The beams and columns were rigidly connected and the infill plate was considered to be connected directly to the beams and columns. Initial imperfections were applied in the model to help initiate buckling in the infill plate and development of the tension field. The infill plate was taken to have an initial imperfection pattern corresponding to the first buckling mode of the plate wall with a peak amplitude of 1 mm. Thus, an eigenvalue buckling analysis was first run on the SPSW (with a flat infill plate) to extract the first buckling mode.

The finite element model thus developed was validated by comparing a quasi-static cyclic loading test results [7] of an unstiffened steel plate shear panel with a centrally placed circular opening with the corresponding analysis results. As explained in [7], the shear panel was 450 mm wide and had a height ($d_p$) of 300 mm. The centrally placed circular opening had a diameter of 60 mm and the plate thickness was 0.83 mm. A quasi-static cyclic loading was applied on the test specimen by applying tensile forces along one panel diagonal. The cyclic loading was repeated to obtain four complete cycles of hysteresis curves. Details of the test specimen and loading history are presented elsewhere [7]. Nonlinear finite element analysis was carried out for the test specimen. For simplicity the framing members were modeled using beam element (ABAQUS element B31). Fig. 4(a) shows the finite element mesh for the steel plate shear panel tested by Roberts and Sabouri-Ghomi [7]. The hysteresis curves generated from the finite element analysis is compared with the test results in Fig. 4 (b). An excellent agreement is observed between analysis and test results. The peak load observed during the test is underestimated only by 4%. Also, the finite element model has previously been validated for several quasi-static tests and one dynamic test on solid SPSWs [16] and it was observed that the developed FE model can capture all the essential parts of load–displacement behavior of SPSW.

The validated finite element model was then used to model and analyze all the selected perforated shear walls. The shear walls were assumed to have hinge supports at the bases of the columns. The hinges at the bases were modeled using rigid beam connections (BEAM-type multi-point constraints in ABAQUS) between the nodes at the base cross-sections of the columns and a reference node at the center of the column.

All steel members were assumed to have a modulus of elasticity of 200,000 MPa. An elasto-plastic stress versus strain curve was adopted, with a yield strength of 385 MPa for the infill plates, and 350 MPa for the beams and columns. A displacement control solution strategy where the top storey displacement was used as the control parameter was used in this work. A target displacement of 110 mm was selected for all the pushover analyses of the single storey perforated SPSWs.

### 3.3. Pushover analysis and results

For all three aspect ratios, perforated steel plate shear walls with the nine different perforation diameters were modeled and analyzed. For each aspect ratio, a SPSW with a solid infill plate was also analyzed to compare the behavior with perforated SPSWs. It may be more rational, instead of comparing the total shear strengths, which include both the strength of the infill plate and that of the boundary frame, to compare only the infill plate strengths with that for different perforation diameters. Thus, for all three aspect ratios, FE model consisting of only the rigid frame of the SPSW was also analyzed Table 2 presents the base shears for the selected single storey SPSWs with solid infill plate and without any infill plate (bare frame). Table 2 also presents the design base shear for the selected single storey SPSWs. It is observed from Table 2 that the selected single storey SPSWs have significantly high overstrength. This is mainly due to use of larger than required infill plate thickness. When higher overstrength infill plates are used, steel plate shear walls require very heavier boundary columns to be designed to achieve full capacity of the infill plates. Base shears for all the perforation cases are presented in Table 3. As expected for any perforation diameter, the total base shear increases with an increase in aspect ratio of the shear wall. Also,

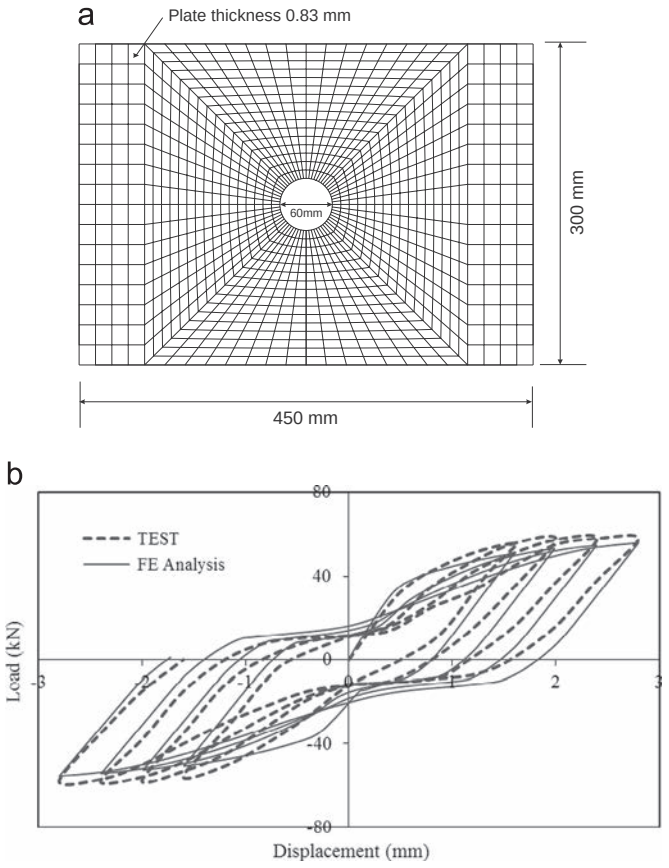


**Fig. 4.** Comparison of hysteresis curves with test results of Roberts and Sabouri-Ghomi [7]: (a) FE mesh; and (b) Hysteresis curves.

**Table 2**
Total base shear of SPSWs with and without solid infill plates.

| Aspect ratio | Plate thickness (mm) | Base shear from pushover analysis (kN) | | Design base shear (kN) |
|---|---|---|---|---|
| | | SPSW with solid infill plate | SPSW frame (no infill plate) | |
| 1.0 | 3 | 3152 | 1647 | 117.5 |
| 1.0 | 1 | 1184 | 509 | 117.5 |
| 1.5 | 3 | 5519 | 2868 | 117.5 |
| 2.0 | 3 | 9771 | 6269 | 117.5 |

**Table 3**
Total base shear for perforated SPSWs.

| Perforation diameters (mm) | Total shear strength (kN) | | | |
|---|---|---|---|---|
| | Aspect ratios | | | |
| | 1.0 (3 mm plate) | 1.0 (1 mm plate) | 1.5 (3 mm plate) | 2.0 (3 mm plate) |
| 400 | 2893 | 1075 | 5092 | 9378 |
| 500 | 2851 | 1049 | 5074 | 9311 |
| 600 | 2794 | 1015 | 5033 | 9232 |
| 750 | 2723 | 976 | 4945 | 9174 |
| 1000 | 2608 | 923 | 4796 | 9041 |
| 1250 | 2533 | 888 | 4679 | 8926 |
| 1500 | 2467 | 847 | 4563 | 8767 |
| 1750 | 2396 | 812 | 4470 | 8623 |
| 2000 | 2332 | 776 | 4314 | 8475 |

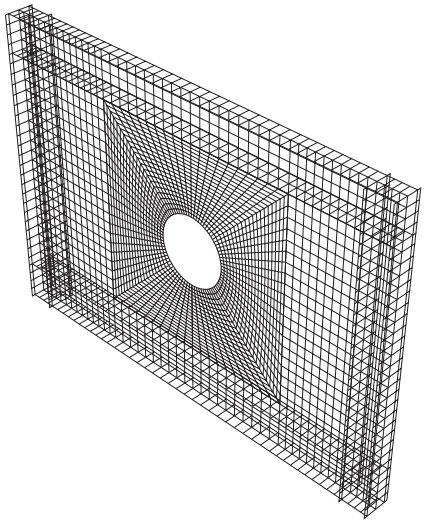

**Fig. 5.** FE mesh for perforated SPSW with aspect ratio 1.5 ($D$=1000 mm).

for any aspect ratio, pushover analysis results show that there is a reduction in the shear strength of the SPSW as the perforation diameter increases. Thus for all the cases considered here, the lowest base shear is observed, 2332 kN, when perforation diameter is 2000 mm and aspect ratio is 1.0. Fig. 5 shows a typical finite element mesh for SPSW with perforation diameter of 1000 mm and an aspect ratio of 1.5. Fig. 6 presents the pushover curves for perforated SPSWs with aspect ratio 1.5.

The pushover analysis results from all the perforation cases were used to evaluate the applicability of Eq. (6) to predict shear strength of centrally placed circular perforation in SPSW. By assuming that the overall SPSW strength can be approximated by the summation of the base frame and the infill plate strengths, it is possible to estimate the infill plate strength by subtracting the bare frame strength from the total strength at the same displacement level. This approximation which does not satisfy the compatibility of deformations at the frame and plate interface for the SPSW and bare frame system has previously been adopted in many research [3,8] and does not have any significant effect in the global behavior of SPSW system. A target displacement of 110 mm is used for all the pushover analysis in this study. Ratios of perforated infill plate strengths to the solid infill plate strength, $V_{op}/V_p$, were calculated for all perforation cases and are presented in Table 4. The ratios of $V_{op}/V_p$ for the all different perforation diameters were plotted against $D/L_p$. As specified earlier, a value of $\alpha$=45° was used in Eq. (6) for the angle of inclination of the tension field for all cases investigated. Fig. 7 presents ratios of perforated infill plate strengths to the solid infill plate strength, as determined from finite element analysis (FEA) for aspect ratio of 1.0. It is observed that Eq. (6) can be used to estimate the shear strengths of perforated infill plates with a reasonable accuracy from a perforation diameter of 400 mm ($D/L_p = 0.12$) to a perforation diameter of 750 mm ($D/L_p = 0.22$). Fig. 8 presents ratios of perforated infill plate strengths to the solid infill plate strength (for Aspect ratio 1.5), as determined from finite element analysis (FEA), compared to the ratios predicted using Eq. (6). Excellent agreement is observed between the FEA results and Eq. (6) when ($0.11 \le (D/L_p) \le 0.24$). It is also observed from Fig. 8 that for aspect ratio of 1.5, Eq. (6) slightly overestimates (less than 4% for the

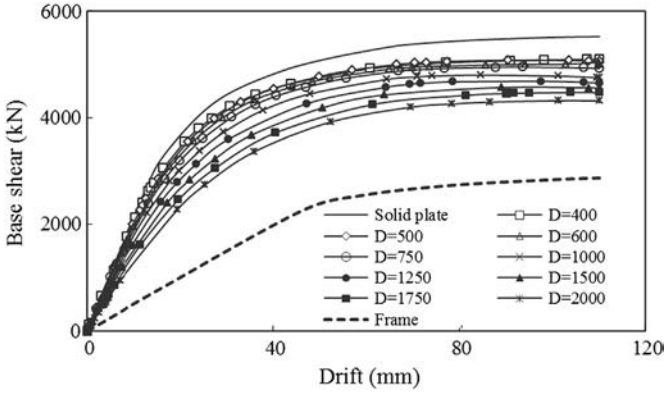


**Fig. 6.** Pushover curves for perforated SPSWs with aspect ratio 1.5.

**Table 4**
Ratios of perforated to solid infill plate strengths.

| Perforation diameters (mm) | $\frac{V_{op}}{V_p}$ from FE analysis | | | |
|---|---|---|---|---|
| | Aspect ratios | | | |
| | 1.0 (3 mm plate) | 1.0 (1 mm plate) | 1.5 (3 mm plate) | 2.0 (3 mm plate) |
| 400 | 0.83 | 0.84 | 0.84 | 0.89 |
| 500 | 0.80 | 0.80 | 0.83 | 0.87 |
| 600 | 0.76 | 0.75 | 0.82 | 0.85 |
| 750 | 0.71 | 0.69 | 0.78 | 0.83 |
| 1000 | 0.64 | 0.61 | 0.73 | 0.79 |
| 1250 | 0.59 | 0.56 | 0.68 | 0.76 |
| 1500 | 0.54 | 0.50 | 0.64 | 0.71 |
| 1750 | 0.50 | 0.45 | 0.60 | 0.67 |
| 2000 | 0.46 | 0.40 | 0.55 | 0.63 |

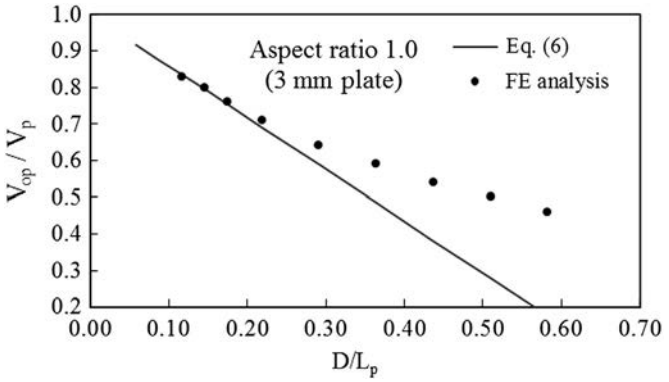


**Fig. 7.** Strength ratios of perforated infill plate to solid infill plate (aspect ratio 1.0).

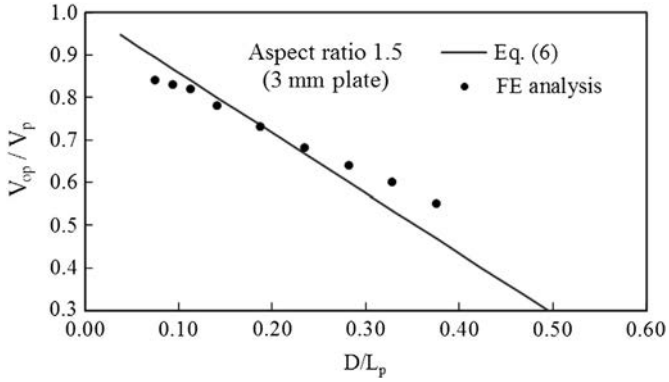


**Fig. 8.** Strength ratios of perforated infill plate to solid infill plate (aspect ratio 1.5).

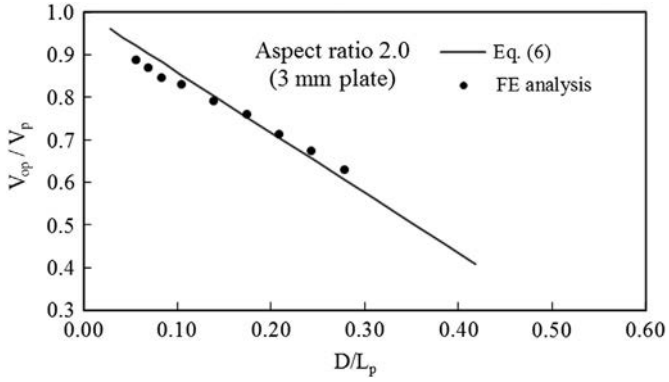


**Fig. 9.** Strength ratios of perforated infill plate to solid infill plate (aspect ratio 2.0).

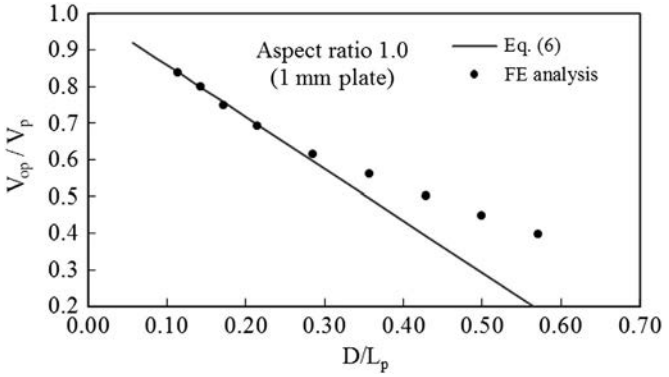


**Fig. 10.** Strength ratios of perforated infill plate to solid infill plate (for 1 mm plate).

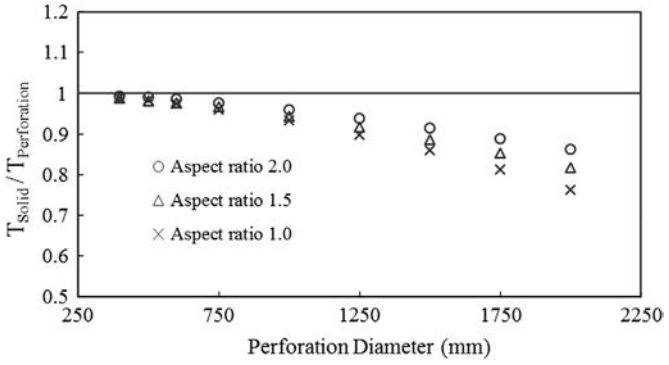


**Fig. 11.** Effect of perforations on period of SPSW.

400 mm diameter and 500 mm diameter case) the value of $V_{op}/V_p$ when the perforation diameters are very small. A slightly overestimation in $V_{op}/V_p$ is always conservative when design of boundary members is of prime interest. This is because in SPSW, according to capacity design, boundary columns are to be *y* designed for the forces from infill plate yielding and plastic hinging of beams at their ends. In case of aspect ratio of 2.0, as shown in Fig. 9, the proposed equation gives excellent predictions of the reduction in shear strength for all the perforation diameters, up to $(D/L_p = 0.28)$, considered here.

As mentioned earlier the selected single storey shear walls have significant overstrenth resulting from the use of commercially available much thicker than required infill plate. To investigate whether the overstrength has any effect on the behavior of SPSW with centrally placed perforations, another single storey SPSW with aspect ratio of 1.0 and a plate thickness of 1 mm, which has lower overstrength, was designed. The selected beam and column sections for the single storey SPSW with 1 mm plate is presented in Table 1. Similar nine different perforation diameters were considered. The perforated SPSWs with were modeled and analyzed in ABAQUS. Finite element models consisting of solid infill plate and only the rigid frame of the SPSW were also analyzed. Table 2 presents the base shears for the selected single storey SPSW (with 1 mm plate) with solid infill plate and without any infill plate (bare frame). Base shears for all the perforation cases are presented in Table 3. As expected, base shears for perforated SPSWs with 1 mm infill plate are significantly lower than those obtained with 3 mm infill plate. Ratios of perforated infill plate strengths to the solid infill plate strength, $V_{op}/V_p$ for the shear wall with 1 mm plate thickness, were calculated for all perforation cases and are presented in Table 4. The ratios of $V_{op}/V_p$ for the all different perforation diameters are plotted against $D/L_p$ in Fig. 10. Excellent agreement is observed between the FEA results and Eq. (6) when $(0.11 \le (D/L_p) \le 0.29)$. Thus, even with a lower overstrenth, Eq. (6) can be used to estimate shear strength of SPSW with centrally placed perforation provided that $D/L_p$ remains higher than 0.11 and lower than 0.29.

Thus, based on the results from all 36 perforation cases, the proposed equation can be used for relating the shear strength of a SPSW with a solid infill plate to an analogous SPSW with a perforated infill plate (with centrally placed circular perforation) provided that the perforation diameter is higher than 10% of the infill plate width but less than 20% of the infill plate width $(0.1 \le (D/L_p) \le 0.2)$. It should be noted that although Canadian design provisions have been used, within the scope of the study, the proposed shear strength equation and the associated conclusions are considered to be general and apply equally to their U.S. and European counterparts.

## 4. Frequency analysis of perforated steel plate shear walls

Frequency analyses of the selected single storey perforated SPSWs (with 3 mm infill plate thickness) with circular perforations in the infill plates were conducted to investigate the effects of perforations on periods of steel plate shear walls. In all frequency analyses, the perforated infill plates were taken to have initial imperfection patterns corresponding to the first buckling modes of the shear walls with peak amplitude of 1 mm. Frequency analyses of single storey SPSWs with solid infill plates were also conducted for all three aspect ratios. The fundamental periods for the single storey SPSWs with solid infill plates were obtained as 0.115 s, 0.139 s and 0.174 s for aspect ratios of 2.0, 1.5 and 1.0 respectively. Fig. 11 presents the results of the frequency analyses of perforated SPSWs. In this figure, the ratio of the first fundamental period for SPSWs with solid infill plates to that for SPSWs with perforated

infill plates are presented for all 27 SPSWs (with 3 mm infill plate thickness) selected in this study. It is observed that perforations in infill plates decrease stiffness of the shear walls and thus increase the fundamental periods of SPSWs. Thus for all three aspect ratios, fundamental periods are highest (in this study) when the perforation diameter is 2000 mm. Also, fundamental periods are higher when the aspect ratio of the SPSW is lower. However, the increase in fundamental period is very small (less than 10%) when the perforation diameter is small, less than 30% of the infill plate width, ($D/L_p < 0.3$).

## 5. Design of boundary columns of perforated steel plate shear walls

As stated earlier, a simple and efficient capacity design method for design of columns of SPSWs with solid infill plates is presented in AISC Steel Design Guide 20 [9]. The method is modified here to include the effects of centrally placed circular perforations in the infill plates. The modifications can be summarized as follows:

(1) For a selected perforation diameter, the ratio of perforated infill plate strength to the solid infill plate strength, $V_{op}/V_p$, is calculated using Eq. (6).
(2) The distributed loads developed from yielding of the perforated infill plates, as shown in the free body diagram in Fig. 12 of a typical column from an n-storey SPSW, can be obtained by multiplying the distributed loads developed from yielding of solid infill plates by $V_{op}/V_p$. Thus, the distributed loads applied to the columns ($\omega_{yci}$ and $\omega_{xci}$) and beams (($\omega_{ybi}$ and $\omega_{xbi}$) and ($\omega_{ybi-1}$ and $\omega_{xbi-1}$)) at any storey $i$ can be determined as

$$\omega_{xci} = (V_{op}/V_p)_i R_y F_y w\,(\sin\,\alpha_i)^2;$$
$$\omega_{yci} = (V_{op}/V_p)_i 0.5 R_y F_y w\,\sin\,2\alpha_i \quad (8)$$

$$\omega_{xbi} = \omega_{xbi-1} = (V_{op}/V_p)_i 0.5 R_y F_y w\,\sin\,2\alpha_i \quad (9)$$

$$\omega_{ybi} = \omega_{ybi-1} = (V_{op}/V_p)_i R_y F_y w(\cos\,\alpha_i)^2 \quad (10)$$

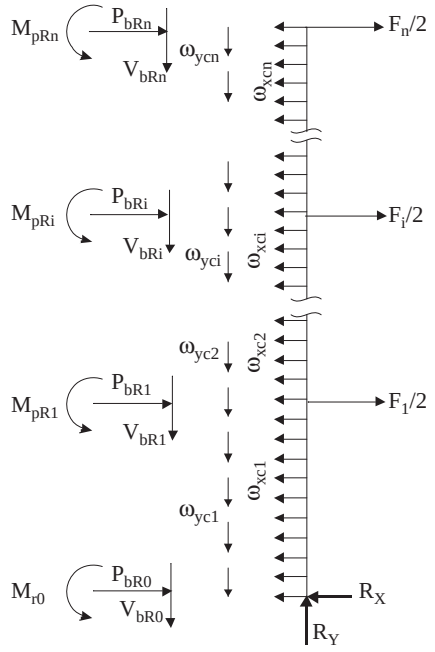


**Fig. 12.** Free body diagram of typical right column of a SPSW.

It is assumed that the distributed loads calculated in this way will act uniformly over the length of beams and columns in every storey.
(3) The beam at any storey $i$ is designed for distributed loads obtained from the difference between the tension forces developed in the infill plates at storey $i$ and $i+1$, namely, $\omega_{bi} = (V_{op}/V_p)_i(\omega_{ybi} - \omega_{ybi+1})$. The distributed loads are then combined with the gravity loads using appropriate load factors.
(4) Axial forces in the beams, $P_b$, can be estimated using the approach outlined in AISC Steel Design Guide 20 [9]. Axial forces are obtained from two sources: the first is due to the inward force from the infill plate applied to the columns, $P_{b(col)}$, and the second is from the difference in the effects of the infill plates above and below the beam, $P_{b(plate)}$. Thus, the axial force in the beam is

$$P_b = P_{b(col)} \pm P_{b(plate)} \quad (11)$$

The axial force at the ends of the beam at storey $i$ is

$$P_{bi} = \left(\omega_{xci}\frac{h_i}{2} + \omega_{xci+1}\frac{h_{i+1}}{2}\right) \pm (\omega_{xbi} - \omega_{xbi+1})\frac{L}{2} \quad (12)$$

At the end where the column is in tension, the above two components of the axial force in the beams are additive.
(5) All the beams are assumed to form a plastic hinge at their ends. The reduced plastic moment capacity at the ends of beam $i$, $M_{pri}$, can be obtained from the approximate equation [17]

$$M_{pri} = 1.18 Z_{xi} F_{yb}\left(1 - \frac{P_{bi}}{A_{bi}F_{yb}}\right) \le Z_{xi}F_{yb} \quad (13)$$

where $Z_{xi}$ is the beam plastic section modulus, $A_{bi}$ is the beam cross-sectional area, and $F_{yb}$ is the beam yield strength.
Using the reduced plastic moment capacities, the shear forces at the ends of beam $i$, $V_{bi}$, can be obtained using the following equation:

$$V_{bi} = \frac{\sum M_{pri}}{L} \pm (\omega_{ybi} - \omega_{ybi+1})\frac{L}{2} \quad (14)$$

where $\sum M_{pri}$ is the summation of the reduced plastic moment capacities at opposite ends of beam $i$.
With all the force components determined for the column free body diagrams, design axial forces for the columns can be easily calculated.
(6) Column moments are estimated storey by storey, assuming they are rigidly connected to the beams at each floor. In every storey, column moments, $M_{col}$, are calculated as the sum of those arising from infill plate tension and those from plastic hinging of the beam, as follows:

$$M_{col,i} = M_{plate,i} + MAX(M_{beam,i}; M_{beam,i-1}) \quad (15)$$

For a column assumed to be fixed against rotation at each end, the moment from the infill plate tension field is

$$M_{plate,i} = \frac{\omega_{xci} h_i^2}{12} \quad (16)$$

where $\omega_{xci}$ is calculated from Eq. (7). For the moment due to plastic hinging in the beam, $M_{beam,i}$ or $M_{beam,i-1}$, one-half of the reduced plastic moment of the beam can be applied to each column segment connected to that beam (i.e., above and below).
Similar to AISC Steel Design Guide 20 [9], the column moments at the top and bottom storey are taken as the moment due to plastic hinging at the ends of the top and bottom beam.

**Table 5**
Seismic forces for selected perforated SPSWs.

| Storey | Seismic design force (kN) | |
|---|---|---|
| | 4-storey | 6-storey |
| 1 | 152 | 105 |
| 2 | 304 | 210 |
| 3 | 456 | 315 |
| 4 | 213 | 420 |
| 5 | | 526 |
| 6 | | 221 |

**Table 6**
Distributed loads from perforated infill plates for 4-storey perforated SPSW.

| Storey | $\alpha$ (deg.) | Loads from yielding infill plates (kN/m) | | |
|---|---|---|---|---|
| | | $\omega_{yc}$ or $\omega_{xb}$ | $\omega_{xc}$ | $\omega_{yb}$ |
| 1 | 41.5 | 418 | 370 | 473 |
| 2 | 41.5 | 418 | 370 | 473 |
| 3 | 41.5 | 418 | 371 | 472 |
| 4 | 42.8 | 420 | 389 | 454 |

**Table 7**
Beam end forces of 4-storey perforated SPSW.

| Beam | $P_{bL}$ (kN) | $P_{bR}$ (kN) | $M_{prL}$ (kN m) | $M_{prR}$ (kN m) | $V_{bL}$ (kN) | $V_{bR}$ (kN) |
|---|---|---|---|---|---|---|
| Base | 1193 | −1193 | 2044 | 2044 | 1910 | −475 |
| 1 | −1407 | −1407 | 951 | 951 | 334 | 334 |
| 2 | −1408 | −1408 | 951 | 951 | 332 | 335 |
| 3 | −1438 | −1448 | 944 | 942 | 279 | 382 |
| 4 | −1937 | 459 | 1966 | 2044 | −591 | 1998 |

**Table 8**
Design column forces for selected perforated SPSWs.

| Storey | 4-storey perforated SPSW | | 6-storey perforated SPSW | |
|---|---|---|---|---|
| | Column axial force (kN) | Column moment (kN m) | Column axial force (kN) | Column moment (kN m) |
| 1 | 9831 | 2044 | 13,920 | 2044 |
| 2 | 7785 | 921 | 11,876 | 921 |
| 3 | 5735 | 921 | 9831 | 921 |
| 4 | 3632 | 2512 | 7784 | 921 |
| 5 | | | 5735 | 917 |
| 6 | | | 3630 | 2513 |

## 6. Design example

One 4-storey SPSW and one 6-storey SPSW were selected to evaluate the performance of the proposed design method. The selected buildings were assumed to have the same plan area (2014 $m^2$) as the building considered earlier. The building has two identical SPSWs to resist lateral forces in each direction. Each shear wall is 5.7 m wide, measured from center to center of columns, with an aspect ratio of 1.5 (storey height of 3.8 m). A dead load of 4.26 kPa was used for each floor and 1.12 kPa for the roof. The live load on all floors was taken as 2.4 kPa. Design seismic loads at every storey were calculated using the equivalent static force procedure of NBC 2010. The base shears for each 4-storey and 6-storey SPSWs were calculated as 1125 kN and 1797 kN respectively. Distribution of the base shears up the height of the selected SPSWs are presented in Table 5. For the design of the perforated steel plate shear walls, an infill plate thickness of 3.0 mm was assumed to be the minimum practical thickness based on handling and welding considerations. For this study, one circular perforation of diameter of 1000 mm was selected in infill plates in every storey. A yield strength of 385 MPa was selected for the infill plates, whereas the yield strength for the beams and columns was taken as 350 MPa. All steel members were assumed to have a modulus of elasticity of 200,000 MPa.

For the perforation pattern selected, using Eq. (6), the value of $V_{op}/V_p$ was calculated as 0.73. The preliminary selection of beams and columns was based on the design loads that were obtained after the first iteration of the proposed method with an assumed tension field inclination angle of 45°. The calculations for the second iteration of the proposed procedure are described in the following only for the 4-storey perforated steel plate shear wall. The distributed forces, obtained from yielding of the infill plates, were obtained from Eqs. (8)–(10) and are presented in Table 6. The angle of inclination of the tension field presented in Table 6 was obtained from the equation in Canadian standard CAN/CSA-S16-09.

Axial forces for the beams of the 4-storey perforated shear wall were calculated using Eq. (12) and are summarized in Table 7. The values of $P_{bL}$ and $P_{bR}$ are the axial force at the beams left and right ends, respectively. The reduced plastic moments for the selected beam sections were calculated using Eq. (13). Using the reduced plastic moment capacity of the beams ($M_{prL}$ and $M_{prR}$), shear forces at the left and at right ends of beams ($V_{bL}$ and $V_{bR}$) were calculated using Eq. (14). Table 7 also tabulates the reduced plastic moments and shear forces at the left and right ends of all beams for the 4-storey perforated SPSW. It should be noted that beam at the base was selected to anchor the tension field developed from the yielding of the infill plate at the lower storey.

Finally, axial forces and bending moments in the boundary columns in every storey were calculated for both 4-storey and 6-storey perforated SPSWs and are presented in Table 8. With the final design forces, column sections were selected for both SPSWs. All the boundary columns selected are class 1 sections and satisfy the column flexibility requirement given by CSA S16-09. It should be noted that class 1 sections have the capacity to attain their plastic moment capacity and subsequent redistribution of the bending moment. The selected perforated SPSWs are shown in Figs. 13 and 16.

Nonlinear pushover analysis were conducted for the selected 4-storey and 6-storey perforated SPSWs and the proposed shear strength equation was evaluated by comparing the shear strengths of the perforated infill plates to the solid infill plates. A target displacement of 500 mm was used for pushover analysis of 4-storey perforated SPSW and for the 6-storey perforated SPSW, a target displacement of 600 mm was selected. It was observed from the pushover analysis that infill plates at the bottom three storeys of the 4-storey perforated SPSW were fully yielded. For the 6-storey perforated SPSW, the bottom 4-storey infill plates were yielded. For this study, ratios of perforated infill plate strengths to the solid infill plate strength, $V_{op}/V_p$, were calculated for the bottom three storeys of both 4-storey and 6-storey perforated SPSWs and are presented in Table 9. It is observed from Table 9 that $V_{op}/V_p$ ratios from the FE analysis are very close to 0.73, predicted from Eq. (6). The maximum difference between the FE analysis result and result from the predicted equation was observed at third storey of the 4-storey perforated SPSW and was approximately 5%. Thus, the proposed shear strength equation, Eq. (6), can be used for calculations of shear strengths of infill plates of multistorey SPSWs with centrally placed circular perforations.

## 7. Comparison with seismic analyses

NBCC 2010 does not specify any number of time histories to use, but it emphasizes the used of spectrum compatible earthquake records. ASCE 7–10 [18] recommends the use of at least three time histories to explore expected seismic performance. Thus seven representative strong earthquakes for Vancouver were selected for the time history response analysis. These are: (1) N–S component of the El Centro earthquake of 1940; (2) Petrolia station record from the 1992 Cape Mendocino earthquake; (3) Nahanni, Canada 1985 earthquake record; (4) Parkfield 1966 earthquake record; (5) San Fernando, California 1971 earthquake record; (6) Kern Country, California 1952 earthquake record; and (7) Borrego Mountain, California 1968 earthquake record. Table 10 presents the different parameters of the selected earthquake ground motions considered for this study. In order to preserve the characteristics of the design response spectrum, Commentary J of NBCC 2010 recommends the use of spectrum compatible earthquake records for time history analysis. Thus, the selected seismic records were modified using the software SYNTH [19] to make them spectrum compatible for Vancouver, Canada. The SYNTH program first computes the spectrum for the real acceleration time history. In order to match the computed spectrum with the target spectrum (design spectrum for Vancouver in this study), the computed spectrum is then raised and suppressed iteratively by corresponding modification of the Fourier coefficients. The spectrum compatible record for the El Centro 1940 earthquake obtained from the program SYNTH, along with the design spectrum, is presented by Bhowmick [1]. Nonlinear time history analyses of the selected perforated SPSWs were performed using ABAQUS [13]. The finite element model includes one steel plate shear wall and a gravity "dummy" column carrying the vertical load supported by half of the leaning columns in the building. The gravity column is made of rigid bar elements and connected to the steel plate shear wall at every storey, with pin-ended rigid links. The gravity "dummy" column is included in the model only to account for P-Delta effects. It is pinned at every floor and its axial stiffness has little, if any, influence on the overall SPSW response. Thus axial stiffness (EA) for the gravity column was selected so that the axial column deformations remain within reasonable limits. Since there will be no moments in that dummy column there is no need to use elements that have end plastic hinge properties. The boundary conditions and material properties are the same as for the single storey SPSWs described earlier. In the finite element analyses, the storey gravity loads were represented as lumped masses on the columns at every floor.

The finite element model described above was used to conduct frequency analysis for the 4-storey and 6-storey perforated SPSWs to determine periods of vibration and corresponding mode shapes. Table 11 presents estimates of the first four in-plane fundamental

**Table 9**
Ratios of perforated to solid infill plate strengths for multistorey SPSWs.

| Storey | 4-storey SPSW | | | 6-storey SPSW | | |
|---|---|---|---|---|---|---|
| | Solid plate shear $V_p$ (kN) | Perforated plate shear $V_{op}$(kN) | $\frac{V_{op}}{V_p}$ | Solid plate shear $V_p$ (kN) | Perforated plate shear $V_{op}$ (kN) | $\frac{V_{op}}{V_p}$ |
| 1 | 3023 | 2246 | 0.74 | 3031 | 2244 | 0.74 |
| 2 | 2991 | 2187 | 0.73 | 3057 | 2213 | 0.72 |
| 3 | 3013 | 2065 | 0.69 | 2930 | 2079 | 0.71 |

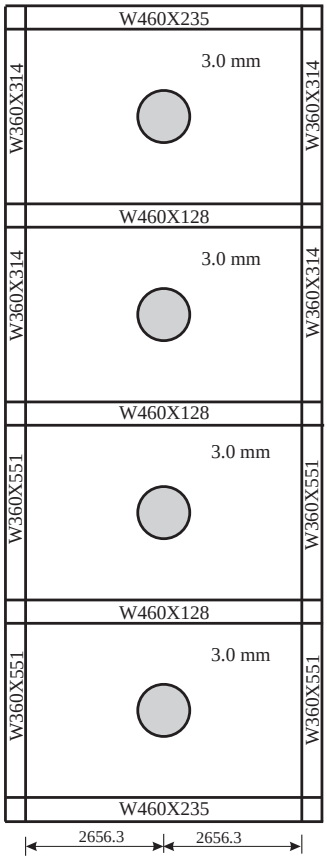


**Fig. 13.** 4-storey perforated SPSW.

**Table 11**
Periods of selected perforated SPSWs.

| Mode | Periods 4-storey SPSW | | | Periods 6-storey SPSW | | |
|---|---|---|---|---|---|---|
| | Perforated SPSW | Solid SPSW | NBC 2010 | Perforated SPSW | Solid SPSW | NBC 2010 |
| 1st | 0.652 | 0.620 | 0.385 | 1.07 | 1.03 | 0.522 |
| 2nd | 0.233 | 0.223 | | 0.352 | 0.340 | |
| 3rd | 0.154 | 0.150 | | 0.206 | 0.200 | |
| 4th | 0.138 | 0.134 | | 0.159 | 0.154 | |

**Table 10**
Description and peak ground motion parameters for selected ground motions.

| Rec. no. | Earthquake | Date | Mag$^n$ | Site | Max. Acc. A (g) | A/V |
|---|---|---|---|---|---|---|
| 1 | Imperial Valley California | May 18, 1940 | 6.6 | El Centro | 0.348 | 1.04 |
| 2 | Cape Mendocino, California | April 25,1992 | 7.1 | Petrolia | 0.59 | 1.2 |
| 3 | Nahanni, Canada | December 23, 1985 | 6.9 | Site 1, Iverson | 1.10 | 2.38 |
| 4 | Parkfield, California | June 27, 1966 | 5.6 | Cholame, Shandon No. 5 | 0.434 | 1.70 |
| 5 | San Fernando, California | February 9, 1971 | 6.4 | Hollywood Storage P.E. Lot, L.A. | 0.211 | 1.0 |
| 6 | Kern County, California | July 21, 1952 | 7.6 | Taft Lincoln School Tunnel | 0.179 | 1.01 |
| 7 | Borrego Mountain. California | April 08, 1968 | 6.5 | San Onofre SCE Power Plant | 0.046 | 1.1 |

**Table 12**
Maximum inelastic response parameters for perforated shear walls.

| Earthquake records | 4-storey SPSW | | | 6-storey SPSW | | |
|---|---|---|---|---|---|---|
| | Roof displacement (mm) | Column forces at the base | | Roof displacement (mm) | Column forces at the base | |
| | | Axial force (kN) | Moment (kN m) | | Axial force (kN) | Moment (kN m) |
| El Centro 1940 | 113 | 7531 | 1701 | 188 | 10,693 | 1641 |
| Petrolia 1992 | 156 | 8489 | 1743 | 215 | 10,806 | 1629 |
| Nahanni 1985 | 136 | 8203 | 1757 | 226 | 11,366 | 1690 |
| Parkfield 1966 | 106 | 7388 | 1569 | 159 | 10,267 | 1524 |
| San Fernando 1971 | 100 | 7551 | 1457 | 224 | 11,330 | 1731 |
| Kern County 1952 | 111 | 7425 | 1609 | 168 | 9811 | 1606 |
| Borrego Mtn. 1968 | 115 | 7597 | 1740 | 185 | 10,316 | 1694 |

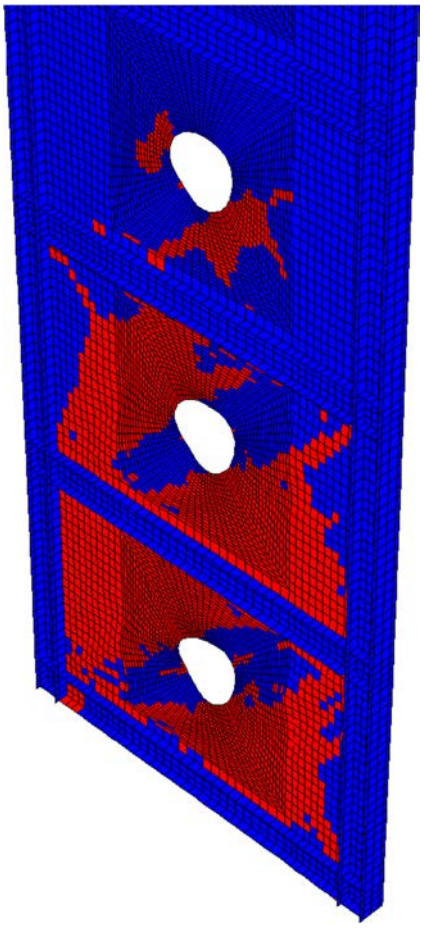

**Fig. 14.** FE mesh of 4-storey SPSW (only the critical portion) under El Centro earthquake at maximum base shear. (For interpretation of the references to color in this figure, the reader is referred to the web version of this article.)

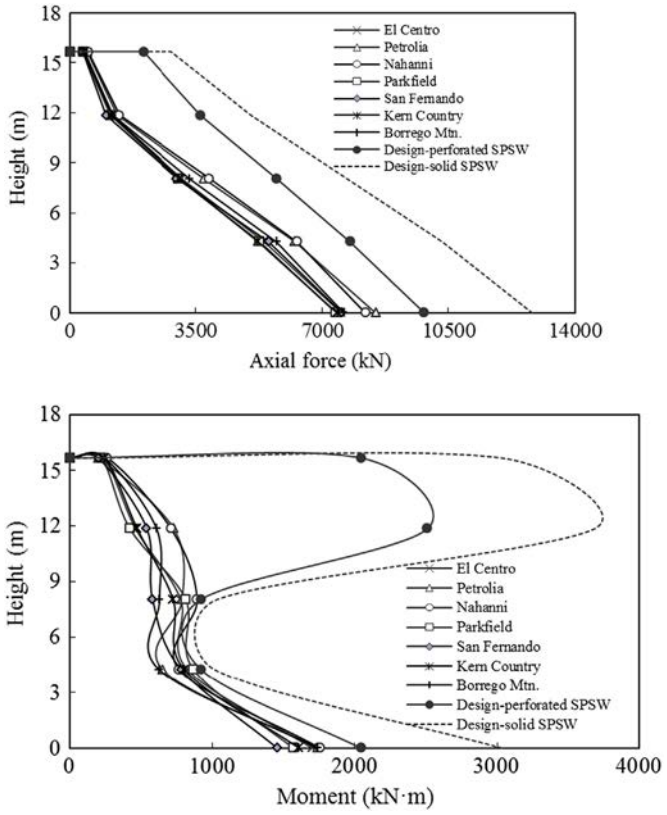


**Fig. 15.** Peak column axial forces and moments for 4-storey perforated SPSW.

periods for both shear walls. NBCC 2010 provides the following empirical expression for estimation of fundamental period of SPSW:

$$T = 0.05(h_n)^{3/4} \quad (17)$$

where $h_n$is the height of the building in meters. Table 11 shows that the computed fundamental period of the 6-storey steel shear wall is 2.05 times larger than the NBC 2010 estimate. For the 4-storey steel plate shear wall the computed fundamental period is 1.7 times the NBC 2010 estimate. Thus, the code specified empirical expression for fundamental period provides a higher spectral acceleration and so is a conservative estimate. Frequency analyses of both 4-storey and 6-storey SPSWs with solid infill plates were also conducted and the results are presented in Table 11. It is observed from Table 11 that the difference between fundamental periods of both 4-storey and 6-storey perforated SPSWs with those with no perforations (solid infill plates) are less than 5%.

Nonlinear dynamic analyses were performed for the two selected shear walls for seven spectrum compatible seismic records for Vancouver, Canada. A damping ratio of 5% in Rayleigh proportional damping with first two modes of vibration was selected for all the seismic analyses. Table 12 presents peak roof displacements for both 4- and 6-storey perforated SPSWs for all the seven seismic records. Table 12 also presents the peak seismic demand (axial forces and column moments) for columns at the base for all seven earthquakes considered in this study. It was observed from the seismic analysis that the selected perforated shear walls behave in a stable and ductile manner.

Fig. 14 shows (the critical portion is only presented) the state of the 4-storey perforated SPSW at the time when the shear at the

base of the wall is maximum for El Centro earthquake record. It was observed that yielding (as shown in red color in FE mesh) is only in the first three infill plates, while the boundary frames remained essentially elastic with the exception of some yielding at the ends of beam at the base. Thus, for this wall, seismic energy was dissipated through yielding in the infill plates. Figs. 15 and 18 present the envelopes of absolute maximum column axial forces and column moments obtained from the seismic analyses. It is observed that for both perforated shear walls, for all ground motions, the axial forces in every storey are lower than the design axial forces obtained from the proposed method. For 4-storey perforated SPSW the maximum column axial force developed at the base from the time history analyses, 8489 kN for the Petrolia 1992 earthquake record, is 13.6% lower than the proposed design axial force, 9831 kN. Fig. 15 also shows that the peak seismic demand for flexure at the base of the columns of 4-storey SPSW, 1757 kN m for the Nahanni, 1985 earthquake record is lower than the proposed design moment of 2044 kN m. Also, the design column moments for the upper stories are much larger than the column moments determined from the seismic analyses.

This occurs because of the assumption made in the capacity design method that plastic hinges form at the ends of all beams. Plastic hinges at the ends of the beams were not observed to form during the seismic analyses of the 4-story perforated SPSW. Thus, proposed design column moments were found to be conservative, as expected.

Fig. 17 shows (the critical portion is only presented) the extent of yielding in the bottom four storeys of the 6-storey perforated SPSW, when the base shear is at its maximum value for El Centro earthquake record. It was observed that yielding is mainly in the first four infill plates. There were some yielding at the ends of beams at base, first, and second storeys. The maximum column axial force developed at the base from the time history analyses as shown in Fig. 18, 11,366 kN for the Nahanni 1985 earthquake record, is 18.3% lower than the proposed design axial force, 13920 kN. Also, the peak seismic demand for flexure at the base of the columns, 1731 kN · m for the San Fernando 1971 earthquake record, is 15.3% lower than the proposed design moment of 2044 kN · m. As expected, proposed design column moments of 6-storey perforated SPSW were found to be conservative.

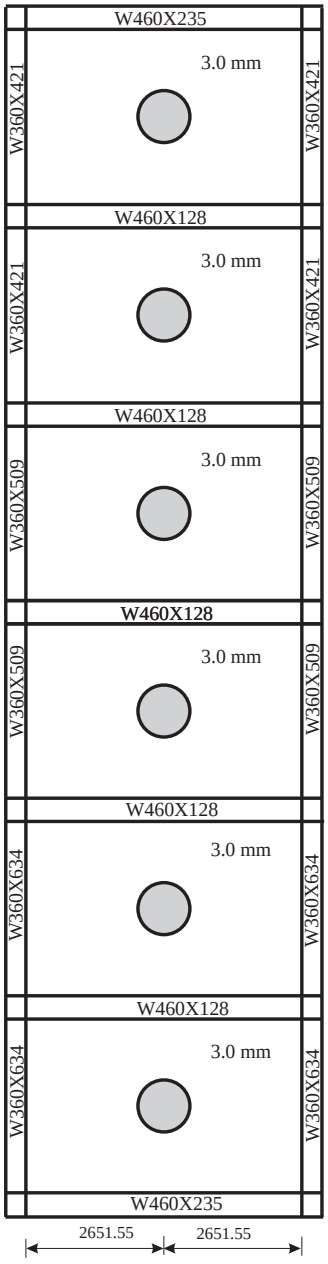


**Fig. 16.** 6-storey perforated SPSW.

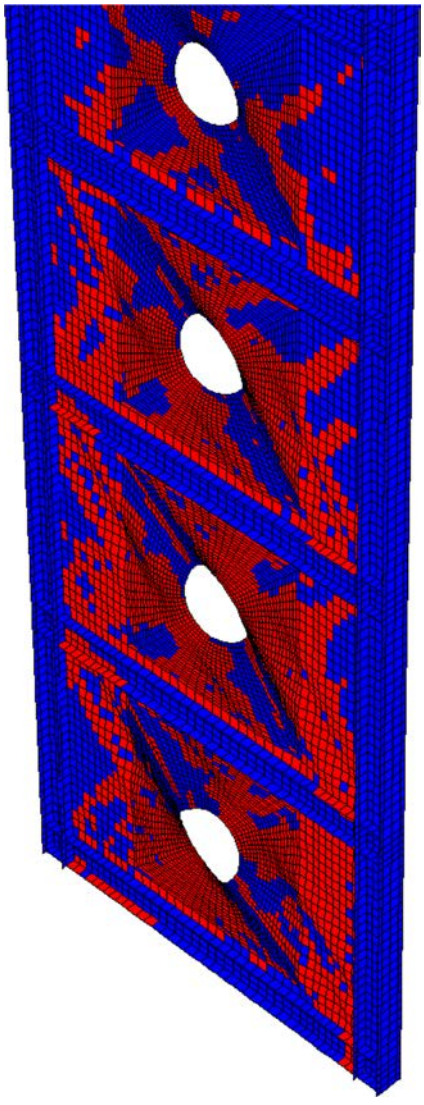

**Fig. 17.** FE mesh of 6-storey SPSW (only the critical portion) under El Centro earthquake at maximum base shear.

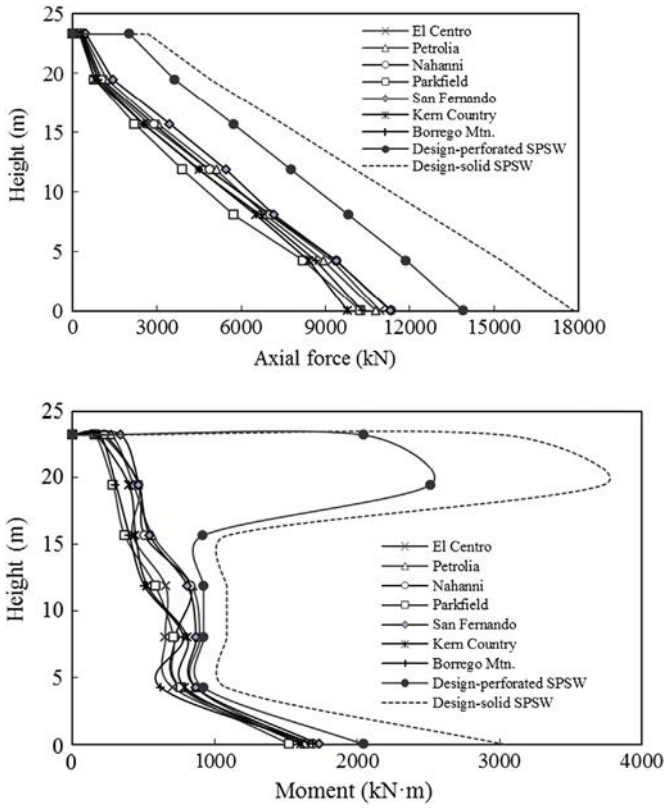


**Fig. 18.** Peak column axial forces and moments for 6-storey perforated SPSW.

One of the objectives of introducing perforations into the infill plates was to reduce the overstrength and, thereby, reduce the design forces for capacity design of the boundary members of the SPSWs. To demonstrate how perforations help reduce the design forces, design forces were calculated for the same 4-storey and 6-storey SPSWs with solid infill plates, following the capacity design method presented in the AISC Steel Design Guide 20. Beam sections in every storey for the 4-storey and 6-storey SPSWs with solid infill plates were the same as the perforated SPSWs, except the beams at the base and top storey, which was selected asW530 $\times$ 300 to resist the yield capacity of the full infill plates.

The design forces calculated for the 4-storey and 6-storey SPSWs with solid infill plates are compared with the design forces for SPSWs with perforated infill plates in Figs. 15 and 18. It is observed that the design column forces in every storey of the perforated SPSWs are lower than those for the SPSW with no perforations (solid). The design column axial force at the base of the 4-storey perforated SPSW, 9831 kN, is 23% lower than the design axial force for the SPSW with no perforations. For 6-storey SPSW, the design column axial force at the base, 13920 kN, is 22% lower than the design axial force, 17,865 kN for the SPSW with no perforations. Figs. 15 and 18 also show that the maximum bending moment at the base of the column of the perforated SPSWs, 2044 kN m, is 33% lower than the design moment for the SPSW with no perforations. Thus the strength of the SPSW can be significantly weakened by introducing circular perforations in the infill plates.

## 8. Conclusions

A series of finite element analyses of unstiffened SPSWs with different perforation diameters and aspect ratios was performed. The analyses show that the shear strength of an infill plate with a centrally placed circular perforation can be calculated by reducing the shear strength of the solid infill plate by the factor given by Eq. (6). The equation was found to give excellent predictions of reduced shear strengths of SPSWs with different perforation diameters and different infill plate aspect ratios provided that the perforation diameter remains within 10–20% of the infill plate width ($0.1 \leq (D/L_p) \leq 0.2$).

A procedure for calculating the design force effects for columns of SPSWs with centrally placed circular perforations in the infi plates is presented. Design column moments and axial forces from the proposed procedure were shown to agree very well with the results of nonlinear seismic analyses of one 4-storey and one 6-storey SPSWs with circular perforations in the infill plates. Furthermore, the advantages of having perforations in the infill plates were demonstrated through nonlinear seismic analysis.

The increase in fundamental period due to the presence of a centrally placed perforation in the infill plate is small and can, in general, be neglected, when the perforation diameter is small. Thus, the fundamental period obtained from SPSWs with solid infill plates can be used for seismic design of similar SPSWs with centrally placed circular perforations.

It is recognized that the proposed shear strength equation for centrally placed perforated SPSW and the conclusion about fundamental period are obtained from nonlinear analysis of limited number of perforated shear walls. Thus, it is suggested that the proposed shear strength equation and the associated conclusions be re-examined with more analysis results of perforated SPSWs with a variation in geometry.

## Acknowledgement

This work was supported by the Faculty of Engineering and Computer Science, Concordia University, Montreal, Canada. Their support is gratefully acknowledged.

## References

[1] Bhowmick AK, Driver RG, Grondin GY. Nonlinear seismic analysis of steel plate shear walls considering strain rate and P-delta effects. J Constr Steel Res 2008;65(5):1149–59.
[2] Berman JW, Bruneau M. Experimental investigation of light-gauge steel plate shear walls. ASCE J Struct Eng 2005;131(2):259–67.
[3] Vian D, Bruneau M. Steel plate shear walls for seismic design and retrofit of building structures. Buffalo, N.Y.: State University of New York at Buffalo; 2005 (Technical report MCEER-05-0010).
[4] Hitaka T, Matsui C. Experimental study on steel shear walls with slits. ASCE J Struct Eng 2003;129(5):586–95.
[5] Cortes G, Liu J. Experimental evaluation of steel slit panel–frames for seismic resistance. J Constr Steel Res 2011;67(2):181–91.
[6] Xue M, Lu L-W. Interaction of infilled steel shear wall panels with surrounding frame members. In: Proceedings of the 1994 annual task group technical session, structural stability research council: reports on current research activities. Lehigh University, Bethlehem, PA; 1994.
[7] Roberts TM, Sabouri-Ghomi S. Hysteretic characteristics of unstiffened perforated steel plate shear panels. Thin Walled Struct 1992;14:139–51.
[8] Purba RH, Bruneau M. Finite element investigation and design recommendations for perforated steel plate shear walls. ASCE J Struct Eng 2009;135(11):1367–76.
[9] Sabelli R, Bruneau M. Steel design guide 20: steel plate shear walls. Chicago, IL: American Institute of Steel Construction; 2007.
[10] Canadian Standards Association. CAN/CSA-S16-09. Toronto, Ontario, Canada: Limit States Design of Steel Structures; 2009.
[11] AISC. Seismic provisions for structural steel buildings. Chicago, IL: American Institute of Steel Construction; 2010.
[12] Thorburn LJ, Kulak GL, Montgomery CJ. Analysis of steel plate shear walls. Structural Engineering Report no. 107. Edmonton, AB: Department of Civil Engineering, University of Alberta; 1983.
[13] Hibbitt Karlsson, Sorensen. ABAQUS/standard user's manual. Version 6.7. Pawtucket, RI: HKS Inc.; 2007.
[14] NBCC. National Building Code of Canada. Ottawa, ON, Canada: National Research Council of Canada (NRCC); 2010.

[15] Shishkin JJ, Driver RG, Grondin GY. Steel plate shear walls using the modified strip model.". Structural Engineering Report no. 261. Edmonton, Canada: Department of Civil and Environmental Engineering, University of Alberta; 2005.
[16] Bhowmick AK, Grondin GY, Driver RG. Performance of type D and type LD steel plate walls. Can J Civil Eng 2010;37(1):88–98.
[17] Bruneau M, Whittaker AS, Uang CM. Ductile design of steel structures. New York: McGraw-Hill; 1998.
[18] ASCE 7-10. Minimum design loads for buildings and other structures. USA: American Society of Civil Engineers, Structural Engineering Institute; 2010.
[19] Naumoski N. Program SYNTH-generation of artificial accelerogram history compatible with a target spectrum. User's manual. Ottawa, ON, Canada: Department of Civil Engineering, University of Ottawa; 2001.